ACS APPLIED MATERIALS & INTERFACES

Research Article

www.acsami.org

Efficient Poly(*N*-3-hydroxypropyl)aspartamide-Based Carriers via ATRP for Gene Delivery

Yun Zhu,[†] Gu-Ping Tang,[‡] and Fu-Jian Xu*,[†]

[†]State Key Laboratory of Chemical Resource Engineering, Key Laboratory of Carbon Fiber and Functional Polymers, Ministry of Education, Beijing University of Chemical Technology, Beijing 100029 China

[‡]Institute of Chemical Biology and Pharmaceutical Chemistry, Zhejiang University, Hangzhou, 310028, P. R. China

ABSTRACT: High-molecular-weight comb-shaped cationic copolymers have been of interest and importance as nonviral gene delivery carriers. Poly(DL-aspartamide)-based biomaterials with good degradability and excellent biocompatibility could be used as the potential backbones of gene vectors. In this work, atom transfer radical polymerization (ATRP) was proposed to prepare the biocleavable and biodegradable comb-shaped poly(*N*-3-hydroxypropyl)aspartamide (PHPA)-based gene carriers. The bioreducible ATRP initiation sites were first introduced onto PHPA backbones. Then, the well-defined comb-shaped vectors (SS-PHPDs) consisting of degradable PHPD backbones and disulfide-linked cationic P(DMAEMA) side chains were produced for gene delivery. The P(DMAEMA) side chains were readily cleavable from the backbones under reducible conditions. The degradability of PHPA backbones would benefit the final removal of the gene carriers from the body.

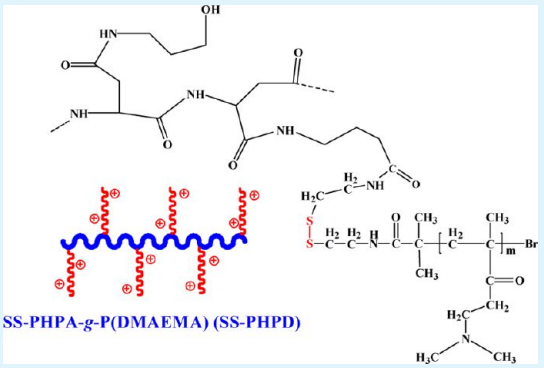

KEYWORDS: *gene delivery, bioreducible, biodegradable, P(DMAEMA), PHPA, ATRP*

INTRODUCTION

Successful gene therapy depends on the design of gene delivery vectors with low cytotoxicity and high transfection efficiency.[1−3] Polycations as the major type of nonviral vectors usually contain primary, secondary, tertiary or quaternary amino groups. Under physiological conditions, polycations can spontaneously condense negatively charged DNA into compact nanocomplexes, reduce the electrostatic repulsion between DNA and cell surfaces, protect plasmid DNA from enzymatic degradation by nucleases, and facilitate cellular transfection. Many kinds of polycations, including polyethylenimine (PEI),[3] poly(tertiaryamine methacrylate),[4] dendrimer polycation,[5,6] and polysaccharide-based cationic carriers[7,8] have been reported to be capable of gene delivery. In general, high-molecular-weight polycations show high transgene expression, but a devastating toxicity. Low-molecular-weight cationic polymers display much lower toxicity, yet suffer from poor transfection activity.

Recently, high-molecular-weight comb-shaped cationic copolymers, where low-molecular-weight polycation side chains were linked onto a long backbone, have emerged as a new leading class of transfection reagents.[9−12] Atom transfer radical polymerization (ATRP) is a recently developed 'controlled' radical polymerization method, which has been used to prepare well-defined graft copolymers from different backbones.[4,13−16] Recently, several types of well-defined polycations were prepared via ATRP as efficient gene vectors.[4] In particular, the successful ATRP syntheses of comb-shaped copolymers composed of polysaccharide backbones (including chitosan,[9] hydroxypropyl cellulose,[10] and dextran[11]) and cationic poly((2-dimethyl amino)ethyl methacrylate) (or P(DMAEMA)) side chains provide a versatile means for designing advanced polysaccharide-based gene carriers. In comparison with the high-molecular-weight P(DMAEMA) homopolymer, the reported polysaccharide-based gene carriers exhibit much lower cytotoxicity and higher gene transfection efficiency in different cell lines.

More importantly, well-defined bioreducible polymers containing easy intracellular reversible disulfide linkage(s) can also be prepared via ATRP by introducing disulfide groups in polymers.[17−19] The bioreducible polymeric vectors containing disulfide bonds were already proven to be a highly advantageous feature for delivering a variety of nucleic acids.[20−23] It was reported that ATRP was used to prepare the well-defined biocleavable comb-shaped vectors consisting of dextran backbones and disulfide-linked cationic P(DMAEMA) side chains for highly efficient gene delivery.[22] The P(DMAEMA) side chains can be readily cleavable from the backbones under reducible conditions. Further improvement in backbone degradability of such comb-shaped vectors will benefit constructing better gene-delivery systems.

Poly(DL-aspartamide)-based biomaterials play a very important role in the design of novel vectors for both gene and drug delivery, due to its low toxicity, good degradability, and

Received: January 3, 2013
Accepted: February 19, 2013
Published: February 19, 2013

   dx.doi.org/10.1021/am400022q | *ACS Appl. Mater. Interfaces* 2013, 5, 1840−1848

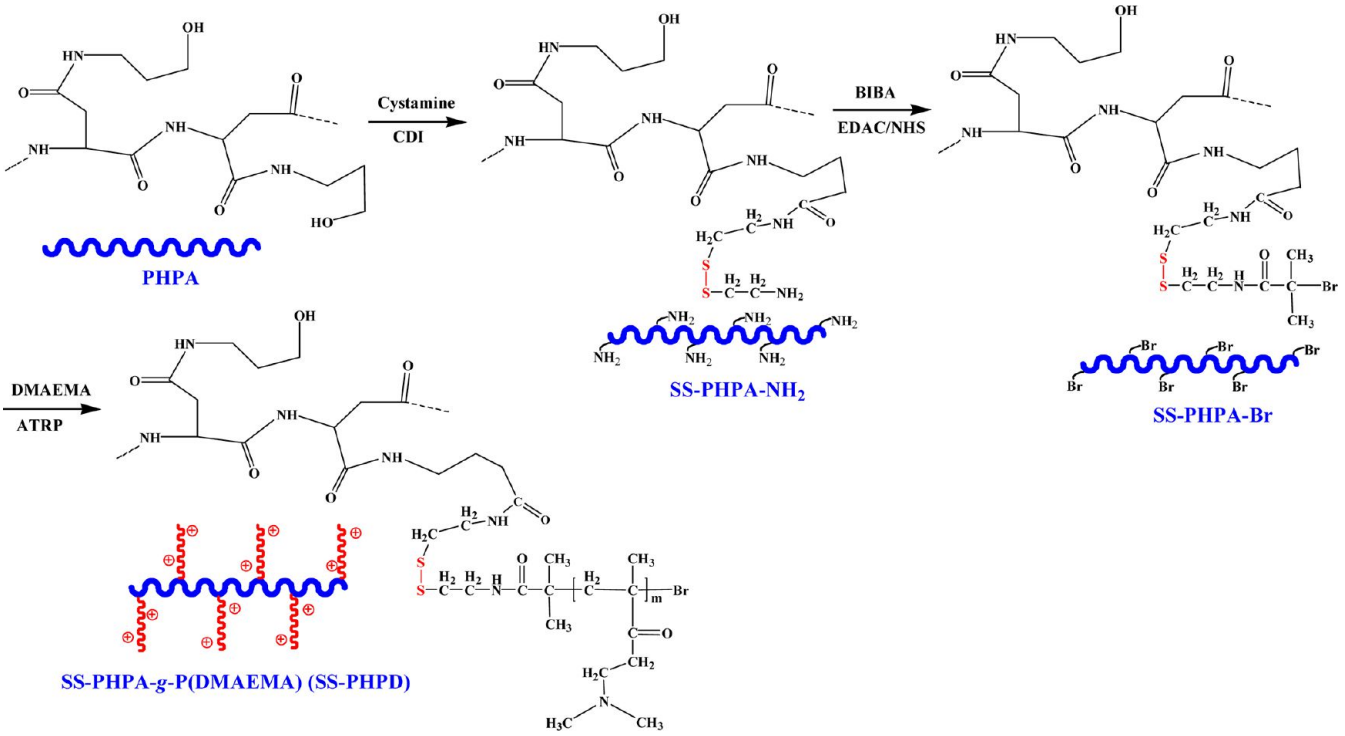

Figure 1. Schematic diagram illustrating the preparation processes of biocleavable and degradable PHPA-*graft*-P(DMAEMA) copolymers via ATRP.

excellent biocompatibility.[12,24−26] To the best of our knowledge, "controlled"/"living" radical graft polymerization techniques have yet to be explored for the design of poly(DL-aspartamide)-based gene carriers. In this work, ATRP was proposed to prepare the biocleavable and biodegradable comb-shaped poly(*N*-3-hydroxypropyl)aspartamide (PHPA)-based gene carriers (Figure 1). The bioreducible ATRP initiation sites were first introduced onto PHPA backbones. Then, the well-defined comb-shaped vectors (SS-PHPDs) consisting of degradable PHPD backbones and disulfide-linked cationic P(DMAEMA) side chains were produced via ATRP for highly efficient gene delivery, where the P(DMAEMA) side chains are readily breakable from the backbones under reducible conditions. The bioreducibility, degradability, and pDNA condensation ability SS-PHPDs have been examined. In vitro cytotoxicity and transfection efficiency of SS-PHPD/pDNA complexes were also investigated.

EXPERIMENTAL SECTION

Materials. Details of the synthesis of α,β-poly(N-3-hydroxypropyl)aspartamide (PHPA, $M_n \approx 2.2 \times 10^4$ g/mol) have been described in our previous publication.[27] The control P-(DMAEMA) homopolymer with about 180 repeat units of DMAEMA was used as one control as before.[11] Branched polyethylenimine (PEI, $M_w \approx 25\,000$ Da), 1,1′-carbonyldiimidazole (CDI, 97%), cystamine dihydrochloride (>98%), 1-ethyl-3-(3-dimethylaminopropyl) carbodiimide hydrochloride (EDAC, 98%), *N*-hydroxysuccinimide (NHS, 98%), α-bromoisobutyric acid (BIBA, 98%), 2-(dimethylamino)ethyl methacrylate (DMAEMA, >98%), 2,2′-byridine (Bpy, 99%), and copper(I) bromide (CuBr, 99%) were obtained from Sigma-Aldrich Chemical Co., St. Louis, MO. DMEAMA were used after removal of the inhibitors in a ready-to-use disposable inhibitor-removal column (Sigma-Aldrich). 3-(4,5-Dimethylthiazol-2yl)-2,5-diphenyl tetrazolium bromide (MTT), penicillin, and streptomycin were purchased from Sigma Chemical Co., St. Louis, MO. HEK293 and COS7 cell lines were purchased from the American Type Culture Collection (ATCC, Rockville, MD).

Synthesis of Biocleavable Comb-Shaped Gene Carriers via ATRP. As shown in Figure 1, the introduction of the bioreducible ATRP initiation sites onto PHPA was carried out in two steps: (1) activation of hydroxyl groups of PHPA in the presence of CDI catalyst to react with cystamine and produce the disulfide bonds-contained dextran (SS-PHPA-NH_2), and (2) reaction of amine groups of SS-PHPA-NH_2 with BIBA in the presence of EDAC and NHS to produce the bromoisobutylryl-terminated PHPA (SS-PHPA-Br). For the activation of hydroxyl groups of PHPA, 0.13 g of CDI and 1.0 g of PHPA were dissolved in 1 and 5 mL of anhydrous DMSO, respectively. The CDI solution was added dropwise at ambient temperature into the PHPA solution. The reaction was allowed to proceed at room temperature for 24 h. Then, 5 mL of DMSO solution containing cystamine dihydrochloride (1.5 g) and triethyleneamine (TEA, 1 mL) was added dropwise into the above CDI-activated PHPA solution. The reaction mixture was stirred at room temperature under an argon atmosphere for 24 h to produce SS-PHPA-NH_2. The final reaction mixture was precipitated and washed with excess diethyl ether, prior to being redissolved in 20 mL of deionized water and dialyzed against deionized water (4 × 5 L) with dialysis membrane (MWCO, 3500 Da) at room temperature for 48 h.

The resultant SS-PHPA-Br was synthesized via the reaction of primary groups of SS-PHPA-NH_2 with BIBA in the presence of EDAC and NHS. BIBA (0.4 g, 2.31 mmol), EDAC (0.46 g, 2.31 mmol), and NHS (0.27 g, 2.31 mmol) were dissolved in 5 mL of DMSO, and then 1 mL of TEA was added. The mixture was stirred at 37 °C for 4 h, and mixed with 1.0 g of SS-PHPA-NH_2 dissolved in 5 mL of DMSO. 0.5 mL of TEA was then added and the reaction mixture was stirred for 48 h at 37 °C. At the end of the reaction, the reaction mixture was precipitated with excess diethyl ether, prior to being redissolved in 20 mL of deionized water and dialyzed against deionized water (4 × 5 L) with dialysis membrane (MWCO, 3500 Da) at room temperature for 24 h, prior to being freeze-dried.

For the preparation of SS-PHPA-*g*-P(DMEAMA) comb-like polymers (named SS-PHPDs), the molar feed ratio [DMAEMA (2 mL)]:[CuBr]:[Bpy] of 100:1:2.5 was used at room temperature in 4 mL of water containing 0.2 g of SS-PHPA-Br. The reaction was conducted in a 25 mL flask equipped with a magnetic stirrer and under the typical conditions for ATRP. DMAEMA, SS-PHPA-Br and Bpy

Table 1. Characterization of the Biocleavable Comb-Shaped Cationic Polymers

sample	reaction time (min)	M_n (g/mol)[b]	PDI[b]	DMAEMA repeat units per side chain		M_n (g/mol)[f]
SS-PHPA-Br[a]		2.23×10^4	1.81			
SS-PHPA-*g*-P(DMAEMA)1 or SS-PHPD1[c]	5	3.25×10^4	1.91	8[d]	11[e]	2.57×10^4
SS-PHPA-*g*-P(DMAEMA)2 or SS-PHPD2[c]	20	5.37×10^4	1.94	25[d]	30[e]	3.12×10^4
SS-PHPA-*g*-P(DMAEMA)3 or SS-PHPD3[c]	40	7.72×10^4	1.71	44[d]	46[e]	4.35×10^4
SS-PHPA-*g*-P(DMAEMA)4 or SS-PHPD4[c]	90	8.62×10^4	1.74	52[d]	56[e]	4.14×10^4

[a]About 15 HPA units of SS-PHPA-Br possess one initiation site or every SS-PHPA-Br chain contains about 8 initiation sites. [b]Determined from GPC results. PDI = weight average molecular weight/number average molecular weight, or M_w/M_n. [c]Synthesized using a molar feed ratio [DMAEMA (2 mL)]:[CuBr]:[bpy] of 100:1:2.5 at room temperature in 4 mL of water containing 0.2 g of SS-PHPA-Br. [d]Determined from M_n and the molecular weights of SS-PHPA-Br (2.23×10^4 g/mol), DMAEMA (157 g/mol), and 8 initiation sites of SS-PHPA-Br. [e]Determined from ^{1}H NMR data. [f]After incubation with DTT for 24 h.

were introduced into the flask containing 4 mL of water, and the reaction mixture was degassed by bubbling argon for 10 min. Then, CuBr was added into the mixture under an argon atmosphere. The flask was then sealed with a rubber stopper under an argon atmosphere. The polymerization was allowed to proceed under continuous stirring at room temperature from 5 to 90 min. The reaction was stopped by diluting with water. The diluted reaction mixture was extensively dialyzed against DDW using a dialysis membrane (MWCO 3500) prior to lyophilization.

Polymer Characterization. The molecular weights of polymers were determined by gel permeation chromatography (GPC), chemical composition by X-ray photoelectron spectroscopy (XPS), and chemical structure by nuclear magnetic resonance (NMR) spectroscopy. GPC measurements were performed on a YL9100 GPC system equipped with a UV/vis detector and Waters Ultrahydrogel 250 (packed with cross-linked hydroxylated polymethacrylate-based gels of 250 Å pore sizes) and Ultrahydrogel Linear (packed with cross-linked hydroxylated polymethacrylate-based gels of different pore sizes) 7.8 × 300 mm columns. The Ultrahydrogel 250 and Ultrahydrogel Linear columns allowed the separation of polymers over the molecular weight ranges of 1×10^3 to 8×10^4 and 1×10^3 to 7×10^6, respectively. A pH 3.5 acetic buffer solution was used as the eluent at a low flow rate of 0.5 mL/min at 25 °C. Monodispersed PEG standards were used to obtain a calibration curve. The XPS measurements were performed on a Kratos AXIS HSi spectrometer equipped with a monochromatized AlK_α X-ray source (1486.6 eV photons), using the same procedures as those described earlier.[11] ^{1}H NMR spectra were measured by accumulation of 1000 scans at a relaxation time of 2 s on a Bruker ARX 300 MHz spectrometer, using D_2O as the solvent. Chemical shifts were referred to the solvent peak, δ = 4.70 ppm. For the bioresponsiveness study, SS-PHPD was treated with 10 mM of DL-dithiothreitol (DTT) for 24 h. The DTT-induced degradation of the disulfide-linked SS-PHPD was analyzed using GPC. For the polymer degradation study, PHPD was dissolved in PBS solution,which was constantly shaken in a 37 °C incubator at 100 rpm. The PHPD solution was withdrawn at different time points for GPC analysis to determine the relative molecular mass of degraded products.

Biophysical Characterization of Polymer/pDNA Complexes. The plasmid (encoding *Renilla* luciferase) mainly used in this work was pRL-CMV (Promega Co., Cergy Pontoise, France), which was cloned originally from the marine organism *Renilla reniformis*. The plasmid DNA (pDNA) was amplified in *Escherichia coli* and purified according to the supplier's protocol (Qiagen GmbH, Hilden, Germany). The purified pDNA was resuspended in tris-EDTA (TE) buffer and kept in aliquots of 0.5 mg/mL in concentration. All polymer stock solutions were prepared at a nitrogen concentration of 10 mM in distilled water. Solutions were filtered via sterile membranes (0.2 μm) of average pore size and stored at 4 °C. The nitrogen in PHPA backbones exists in amide bonds. PHPA backbones cannot complex with DNA and mediate gene transfection. Thus, in this work, comblike polymers to DNA ratios are expressed as molar ratios of nitrogen (N) from P(DMAEMA) species of SS-PHPD to phosphate (P) in DNA (or as N/P ratios). All polymer/pDNA complexes were formed by mixing equal volumes of polymer and pDNA solutions to achieve the desired N/P ratio. Each mixture was vortexed and incubated for 30 min at room temperature. Each cationic polymer was examined for its ability to bind pDNA through agarose gel electrophoresis using the similar procedures as those described earlier.[9−11] The particle sizes and zeta potentials of the polymer/pDNA complexes were measured in triplicate using a Zetasizer Nano ZS (Malvern Instruments, Southborough, MA) and procedures similar to those described earlier.[9−11] The polymer/pDNA complexes were also imaged with the transmission electron microscopy (TEM) (JEOL JEM 2010F).

Cell Viability. The cytotoxicity of the polymeric vectors was evaluated using the 3-(4,5-dimethylthiazol-2yl)-2,5-diphenyl tetrazolium bromide (MTT) assay in HEK293 and COS7 cell lines. They were cultured in Dulbecco's modified eagle medium (DMEM), supplemented with 10% heat-inactivated fetal bovine serum (FBS), 100 units/mL of penicillin and 100 μg/mL of streptomycin at 37 °C, under 5% CO_2, and 95% relative humidity atmosphere. The cells were seeded in a 96-well microtiter plate at a density of 1×10^4 cells/well and incubated in 100 μL of DMEM/well for 24 h. The culture media were replaced with fresh culture media containing serial dilutions of polymers or 10 μL polyplex solutions at various N/P ratios, and the cells were incubated for 24 h. Then, 10 μL of sterile-filtered MTT stock solution in PBS (5 mg/mL) was added to each well, reaching a final MTT concentration of 0.5 mg/mL. After 5 h, the unreacted dye was removed by aspiration. The produced formazan crystals were dissolved in DMSO (100 μL/well). The absorbance was measured using a microplate reader (Spectra Plus, Tecan, Zurich, Switzerland) at a wavelength of 570 nm. The cell viability (%) relative to control cells cultured in media without polymers was calculated from $[A]_{test}/[A]_{control} \times 100\%$, where $[A]_{test}$ and $[A]_{control}$ are the absorbance values of the wells (with the polymers) and control wells (without the polymers), respectively. For each sample, the final absorbance was the average of those measured from six wells in parallel.

Transfection Assay. Transfection assays were performed first using plasmid pRL-CMV as the reporter gene in HEK293 and COS7 cell lines in the presence of serum. In brief, the cells were seeded in 24-well plates at a density of 5×10^4 cells in the 500 μL of medium/well and incubated for 24 h. The comb-shaped polymer/pDNA complexes (20 μL/well containing 1.0 μg of pDNA) at various N/P ratios were prepared by adding the polymer into the DNA solutions, followed by vortexing and incubation for 30 min at room temperature. At the time of transfection, the medium in each well was replaced with 300 μL of fresh normal medium (supplemented with 10% FBS). The complexes were added into the transfection medium and incubated with the cells for 4 h under standard incubator conditions. Then, the medium was replaced with 500 μL of the fresh normal medium (supplemented with 10% FBS). The cells were further incubated for an additional 20 h under the same conditions, resulting in a total transfection time of 24 h. The cultured cells were washed with PBS twice, and lysed in 100 μL of the cell culture lysis reagent (Promega Co., Cergy Pontoise, France). Luciferase gene expression was quantified using a commercial kit (Promega Co., Cergy Pontoise, France) and a luminometer (Berthold Lumat LB 9507, Berthold Technologies GmbH. KG, Bad Wildbad, Germany). Protein concentration in the cell samples was analyzed using a bicinchoninic acid assay (Biorad Lab, Hercules, CA).

Gene expression results were expressed as relative light units (RLUs) per milligram of cell protein lysate (RLU/mg protein).

RESULTS AND DISCUSSION

Synthesis of Biocleavable SS-PHPD Carriers. As shown in Figure 1, some hydroxyl groups of PHPD were converted into bioreducible initiation sites for growing disulfide-linked cationic side chains. The hydroxyl groups of PHPA were first activated by CDI to react with cystamine, producing the disulfide bonds-contained PHPA (SS-PHPA-NH_2). Then, the primary amine groups of SS-PHPA-NH_2 were activated to react with BIBA in the presence of EDAC) and NH), producing the bromoisobutylryl-terminated dextran (SS-PHPA-Br) as multifunctional initiators. Well-defined SS-PHPA-*g*-P(DMEAMA) copolymers (SS-PHPDs) were subsequently synthesized via ATRP of DMAEMA from SS-PHPA-Br. The SS-PHPDs with different lengths of PDMEAMA side chains can be synthesized by varying the ATRP time. Table 1 summarizes the GPC results of SS-PHPD1 (from 5 min of ATRP), SS-PHPD2 (from 20 min of ATRP), SS-PHPD3 (from 40 min of ATRP), and SS-PHPD4 (from 90 min of ATRP). With the increase in reaction time from 5 to 90 min, the M_n of SS-PHPD from GPC increases from 3.25×10^4 to 8.62×10^4 g/mol. In addition, the PDIs of SS-PHPDs are comparable to that of SS-PHPA-Br, indicating that ATRP of DMEAMA is well-controlled.

Polymer Characterization. The chemical compositions of the polymers were first determined by ^{1}H NMR. Figure 2 shows the representative ^{1}H NMR structures of (a) PHPA, (b) SS-PHPA-NH_2, (c) SS-PHPA-Br, (d) SS-PHPD1, and (e) SS-PHPD4. The broad chemical shifts of PHPA in the wide region of 2.6−2.8 ppm are mainly associated with the inner methylidyne and methylene protons adjacent to the ester linkages (*a*, $\underline{CH_2}$-C═O, *a*′, $\underline{CH}$-C═O). The other typical chemical shifts associated with PHPA backbone include peaks ***b*** (δ = 3.17, $\underline{CH_2}$-NH), *c* (δ = 1.6, $\underline{CH_2}$-CH_2), and *d* (δ = 3.6, $\underline{CH_2}$−OH). For SS-PHPA-NH_2, the signal at δ = 2.67 ppm corresponds to the methylene protons adjacent to the disulfide bonds (*e*, $\underline{CH_2}$−S-S). For SS-PHPA-Br, the chemical shift at δ = 1.83 ppm is associated with the methyl protons (*f*, C(Br)-$\underline{CH_3}$) of the 2-bromoisobutyryl groups. To avoid potential gelation and introduce some flexibility onto the comblike cationic copolymers, the SS-PHPA-Br with moderate initiation sites was desired for subsequent comb-shaped copolymers. In this work, based on the ^{1}H NMR data, it was calculated that about 15 HPA units of SS-PHPA-Br possess one ATRP initiation site in the present conditions, or every SS-PHPA-Br chain contains about 8 initiation sites (Table 1). Such prepared SS-PHPA-Br with moderate initiation sites can avoid potential gelation during ATRP. With the increase in reaction time from 5 to 90 min, the total number of DMEAMA repeat units per side chain increases accordingly from 8 to 52, based on the assumption of one initiation site out of every 15 HPA units of SS-PHPA-Br (Table 1). In addition, the concentration of initiation sites can be controlled by adjusting the cystamine/PHPA feed ratio.

The typical ^{1}H NMR spectra of SS-PHPD1 and SS-PHPD4 are shown in panels d and e in Figure 2, respectively. The typical chemical shifts at about 0.95, 1.9, 2.28, and 2.69 ppm are mainly attributable to the (*g*′) C−$\underline{CH_3}$ methyl, (*g*) C−$\underline{CH_2}$ methylene, (*h*′) N−$\underline{CH_3}$ methyl, and (*h*) N−$\underline{CH_2}$ methylene protons of the P(DMAEMA) side chains, respectively. The chemical shift (at δ = 4.13 ppm) was associated with the methylene protons adjacent to the oxygen moieties of the ester linkages (*i*, $\underline{CH_2}$−O−C═O). With the increase in ATRP time,

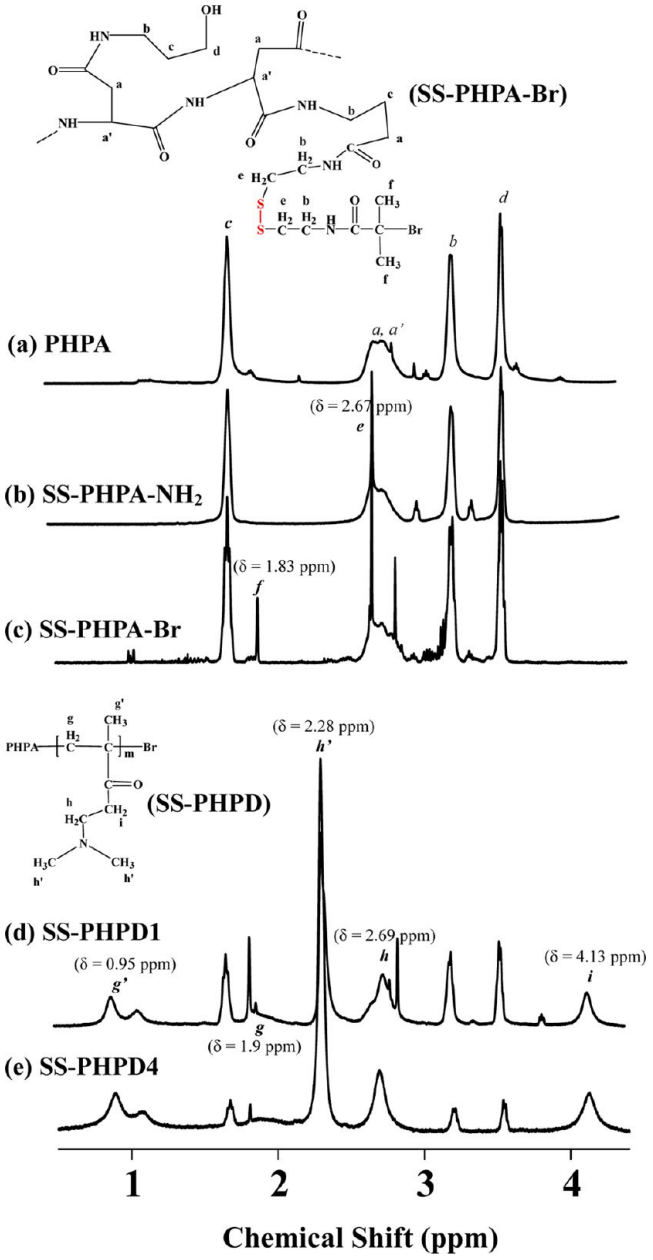

Figure 2. ^{1}H NMR spectra of the (a) PHPA, (b) SS-PHPA-NH_2, (c) SS-PHPA-Br, (d) SS-PHPD1, and (e) SS-PHPD4 in D_2O.

the signal intensities (*b*, *c*, *d*) of SS-PHPD associated with the PHPA backbone decreased substantially, because of the decreased contribution of PHPA to the overall comb polymer structures. From the ^{1}H NMR spectra of SS-PHPDs, the average number of DMAEMA repeat units per side chain was also estimated and summarized in Table 1.

The C 1s core-level XPS spectra of the pristine PHPA, SS-PHPA-NH_2 and SS-PHPA-Br are shown in Figure 3a−c, respectively. The C 1s core-level spectra can be curve-fitted by four peak components with BE's at about 284.6, 285.4, 286.2, and 287.6 eV, attributable to the $\underline{C}$−H, $\underline{C}$−N, $\underline{C}$−O for PHPA (or $\underline{C}$−O/$\underline{C}$−S for SS-PHPA-NH_2 or $\underline{C}$−O/$\underline{C}$−S/$\underline{C}$−Br for SS-PHPA-Br), and NH−$\underline{C}$═O species, respectively. The $\underline{C}$−S peak components were associated with the cystamine species of SS-PHPA-NH_2 and SS-PHPA-Br. The corresponding S 2p (with BE at about 164 eV) core-level spectrum of SS-PHPA-NH_2 is shown in Figure 2b′. The corresponding Br 3d core-

dx.doi.org/10.1021/am400022q | ACS Appl. Mater. Interfaces 2013, 5, 1840−1848

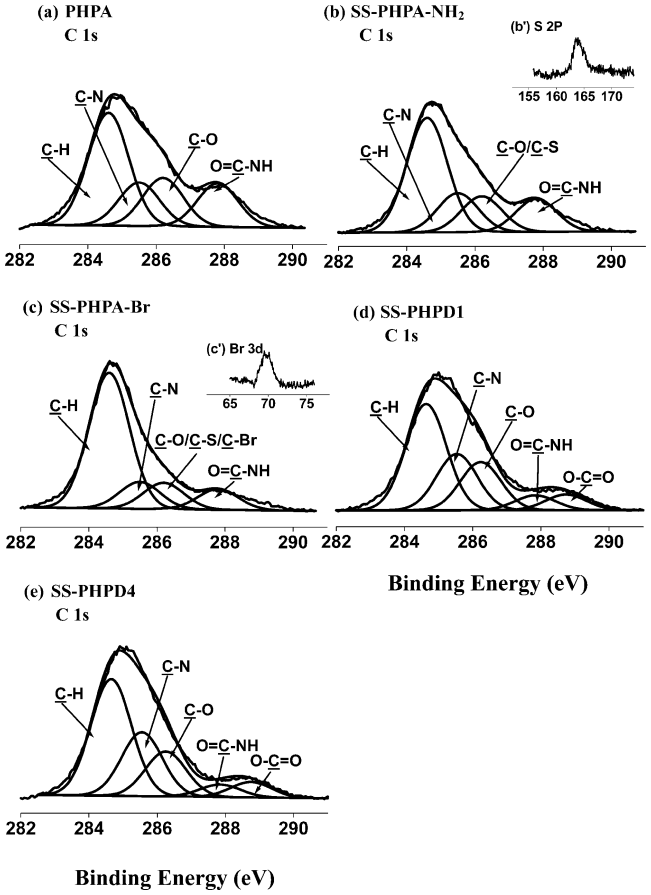

Figure 3. XPS C 1s spectra of (a) PHPA, (b) SS-PHPA-NH_2, (c) SS-PHPA-Br, (d) SS-PHPD1, and (e) SS-PHPD4, (b′) S 2p core-level spectrum of SS-PHPA-NH_2, and (c′) Br 3d core-level spectrum of SS-PHPA-Br.

level spectrum (with BE at about 69 eV) of SS-PHPA-Br is shown in Figure 3c′. The above XPS results also clearly confirmed the successful preparation of SS-PHPA-NH_2 and SS-PHPA-Br. The corresponding core-level spectra of SS-PHPD1 and SS-PHPD4 are shown in d and e in Figure 3, respectively. The C 1s core-level spectra can be curve-fitted into five peak components with BE's at about 284.6, 285.5, 286.2, 287.6, and 288.4 eV, attributable to the C−H, C−N, C−O, O=C−NH, and O=C−O species, respectively. The O=C−O peak was associated with the P(DMAEMA) side chains, which was consistent with the presence of P(DMAEMA).

The disulfide bridge linkages between P(DMAEMA) side chains and PHPA backbones can make SS-PHPD reductively breakable under reducible conditions. To demonstrate the responsiveness, SS-PHPD was treated with 10 mM of DL-dithiothreitol (DTT), analogous to the intracellular redox potential.[28] Such DTT-induced degradation of the disulfide-linked SS-PHPD was demonstrated using GPC analysis (Figure 4). After incubation with DTT for 24 h, the molecular weight of SS-PHPD2 decreased substantially. The significant differences in the aqueous GPC traces of SS-PHPD2 before and after the treatment with DTT clearly showed that the disulfide-linked SS-PHPD was responsive to the reductive agent DTT. After incubation with DTT, the decreased molecular weights of all the SS-PHPD vectors were summarized in Table 1.

Polymer degradation plays an important role in regulating cytotoxicity of polymeric gene vectors and their final removal

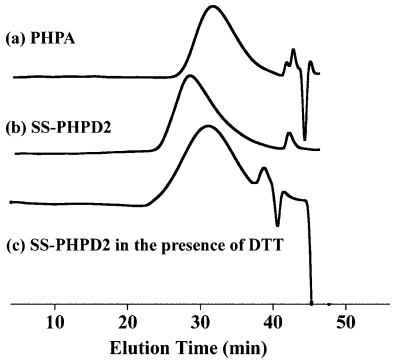

Figure 4. Aqueous GPC traces obtained for (a) PHPA, (b) SS-PHPD2, and (c) SS-PHPD2 in the presence of 10 mM DTT, where the incubation time with DTT was 24 h.

from the body. The polymer degradation was investigated by dissolving SS-PHPD in PBS solution in the presence of DTT which was constantly shaken in a 37 °C incubator. As shown in Figure 5, the M_n of SS-PHPD2 decrease significantly at the

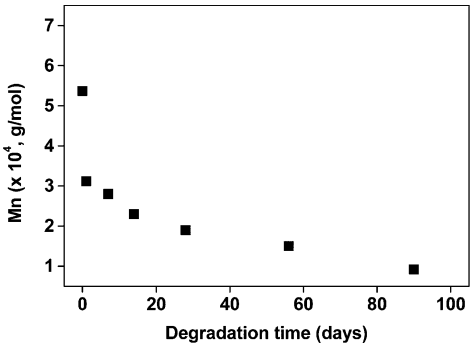

Figure 5. Change of molecular weight of SS-PHPD2 with degradation time in PBS (pH 7.4) in the presence of DTT at 37 °C.

initial stage, mainly due to the rapid detachment of the low-molecular-weight disulfide-linked P(DMAEMA) side chains from the PHPA backbone in the presence of DTT. After the rapid detachment of P(DMAEMA) side chains, SS-PHPD2 entered the gradual degradation state with degradation time, which was mainly attributed to the slow degradation of PHPA backbones.

Biophysical Properties of Polymer/pDNA Complexes. For cellular transfection, the DNA condensation induced by polycation into nanoparticles is a prerequisite for a successful gene delivery system to facilitate cellular uptake. In this work, the ability of the cationic copolymers to condense plasmid DNA (pDNA) into particulate structures was confirmed by agarose gel electrophoresis, particle size and zeta potential measurements, as well as TEM imaging. The formation of the copolymer/pDNA complexes was first analyzed by their electrophoretic mobility on an agarose gel at various nitrogen (N)/phosphate (P) (or N/P) ratios. In this work, for simplicity, comblike SS-PHPA polymers to DNA ratios are expressed as molar N/P ratios of nitrogen from charged P(DMAEMA) species of SS-PHPD to phosphate in DNA. At the given N/P ratios, SS-PHPD possessed similar density of charged groups. Figure 6 shows the gel retardation results of the SS-PHPD/pDNA complexes with increasing N/P ratios, in comparison with that of the branched PEI (25 kDa)/pDNA complexes. SS-PHPD1 compacted pDNA completely at the N/

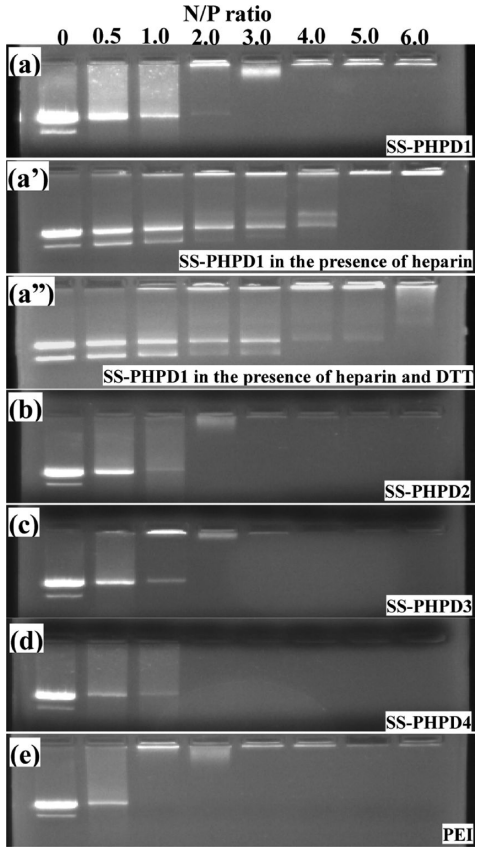

Figure 6. Electrophoretic mobility of plasmid DNA (pDNA) in the complexes of the cationic polymers ((a) SS-PHPD1, (a′) SS-PHPD1 in the presence of heparin as the counter polyanion, (a′′) SS-PHPD1 in the presence of 10 mM DTT and heparin, (b) SS-PHPD2, (c) SS-PHPD3, (d) SS-PHPD4, and (e) PEI) at various N/P ratios. For (a′) SS-PHPD1 in the presence of heparin, and (a′′) SS-PHPD1 in the presence of 10 mM DTT and heparin, the incubation time was 1 h. For SS-PHPD, polymers to DNA ratios are expressed as molar N/P ratios of nitrogen from charged P(DMAEMA) species of SS-PHPD to phosphate in DNA.

P ratios of above 3. Other SS-PHPDs with longer P(DMAEMA) side chains (Table 1) exhibited slightly higher condensation capability and inhibited the migration of pDNA at the N/P ratios of above 2, similar to those of the control PEI (25 kDa), which generally condensed pDNA completely at the N/P ratios of 1.5−2.0.[9−11,22] However, the SS-PHPD vectors possessed bioreducible and biodegradable properties (see below).

As mentioned earlier, the disulfide bridge linkages between P(DMAEMA) side chains and PHPA backbones were responsive to the reductive agent, which can make SS-PHPD breakable under reducible conditions (Figure 4). Such responsiveness may also have significant effects on pDNA release from the complexes under intracellular reducible conditions. The release of pDNA from the SS-PHPD/pDNA complexes at different N/P ratios was studied under the presence of DTT. In the absence of heparin as the counter polyanion, no obvious difference was observed in the electrophoretic mobilities of pDNA in the SS-PHPD/pDNA complexes before and after the treatment with DTT, indicating that the cleavable P(DMAEMA) side chains still could interact with DNA. However, in the presence of heparin, pDNA could be released at the test N/P ratios after the treatment of the SS-PHPD/pDNA complexes with DTT (Figure 6a′′). In the control experiment without the treatment with DTT, pDNA was just released at the relative low N/P ratios from the SS-PHPD/pDNA complexes in the presence of heparin (Figure 6a′). The above phenomena indicated that the cleavage of the short P(DMAEMA) side chains from the PHPD backbone under the reducible condition could lead to the unstable complexes. Such the unstable complexes were readily decondensed via interexchange with heparin polyanions to induce pDNA release. The above results were consistent with those of our earlier work where P(DMAEMA) side chains were disulfide-linked onto dextran backbones.[22] In fact, varieties of negatively charged macromolecules or cellular components (such as mRNA, sulfated sugars, and nuclear chromatin) exist in cells, which can act as competitors to induce pDNA release.[12] The biocleavable nature of SS-PHPDs may greatly facilitate pDNA release in cells, and in turn, could modulate the gene expression in vitro or in vivo.

The particle size and surface charge of complexes are important factors in modulating their cellular uptake. As shown in Figure 7a, all the cationic vectors could efficiently compact

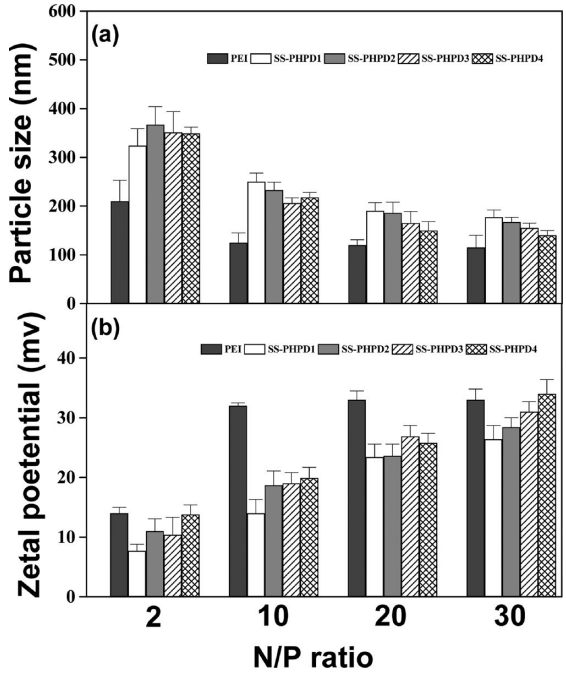

Figure 7. (a) Particle size and (b) zeta potential of the complexes between the cationic polymers (SS-PHPD1, SS-PHPD2, SS-PHPD3, SS-PHPD4, and PEI) and pDNA at various N/P ratios.

pDNA into small nanoparticles. In general, the hydrodynamic size of the complex decreased with increasing N/P ratio. At the N/P ratio of 2.0, loose large aggregates were formed, due to the lower amount of cationic polymers. At higher N/P ratios, all vectors condense pDNA into nanoparticles of around 200 nm. These complexes within this size range can readily undergo endocytosis.[29] Figure 8 shows the representative TEM images of the (a) SS-PHPD1/pDNA and (b) SS-PHPD4/pDNA complexes at a ratio of 20. The images clearly reveal that the compacted complexes exist in the form of nanoparticles. Zeta potential is an indicator of surface charges on the polymer/pDNA nanoparticles. As indicated in Figure 7b, the complex surfaces were positive. The positive net surface charge would

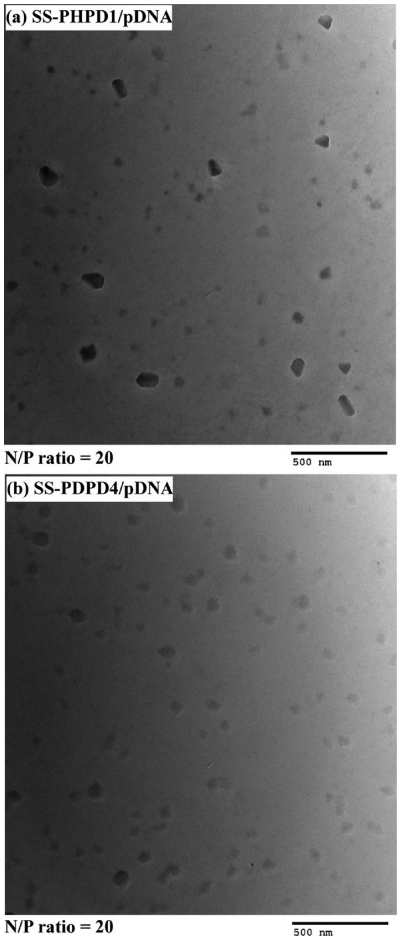

Figure 8. TEM images of the (a) SS-PHPD1/pDNA and (b) SS-PHPD4/pDNA complexes at a N/P ratio of 20.

produce good affinity for anionic cell surfaces and facilitates cellular uptake. In addition, the larger particle sizes and lower charges of SS-PHPD1/pDNA at most N/P ratios were due to its lower condensation capability (Figure 6).

Cell Viability Assay. Cytotoxicity is another important factor to be considered in selecting gene carriers. A successful delivery system should have high transfection efficiency and compromised toxicity. Figure 9 shows the in vitro MTT assay results of cytotoxicity of SS-PHPDs, PHPA, P(DMAEMA), and PEI in (a) HEK293 and (b) COS7 cells. No obvious cytotoxicity was observed for PHPA backbones. All of the cationic polymers exhibit a dose-dependent cytotoxicity effect. SS-PHPDs exhibit increasing toxicity with the increase in ATRP time. Nevertheless, the high-molecular-weight SS-PHPDs (Table 1) exhibit lower toxicity than P(DMAEMA) and PEI. The slopes of the dose-dependent cytotoxicity curves for P(DMAEMA) and PEI are much steeper than those for SS-PHPDs. A high concentration of charged amino groups is always considered an important factor leading to high cytotoxicity. The introduction of the biocompatible PHPD backbones not only results in a lower relative concentration of charged amino groups, but has also imparted biocompatible characteristics to the cationic carriers. In addition, upon cellular uptake, the short biocleavable P(DMAEMA) side chains can be detached from the PHPD backbone, which may also contribute to the lower cytotoxicity of SS-PHPD.

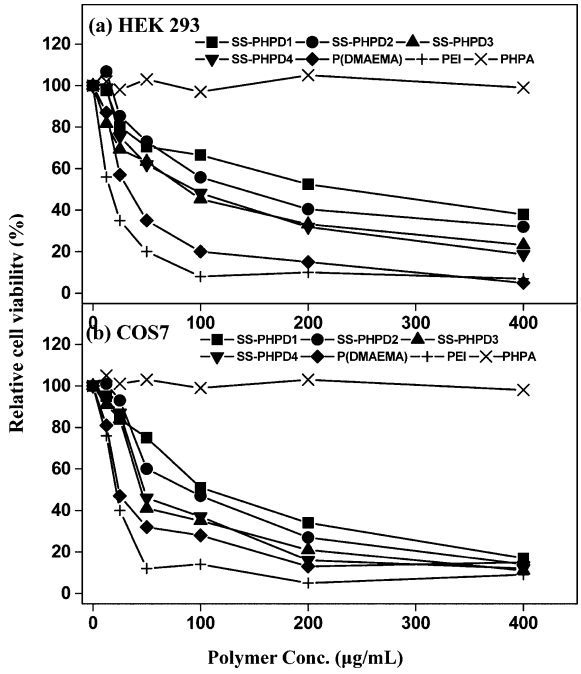

Figure 9. Cell viability assay in (a) HEK293 and (b) COS7 cells with various concentrations of SS-PHPD, SS-PHPD2, SS-PHPD3, SS-PHPD4, P(DMAEMA), PEI, and PHPA. Cell viability was determined by the MTT assay and expressed as a percentage of the control cell culture.

The cell viability of the polymer/pDNA complexes as a function of the N/P ratios was also evaluated in the (a) HEK293 and (b) COS7 cells by using MTT assay (Figure 10). The N/P ratio has a profound impact on the cytotoxicity of complexes. The cell viability of all polymer/pDNA complexes was observed to decrease with increasing N/P ratios. At higher N/P ratios, the transfection formulation contain also free

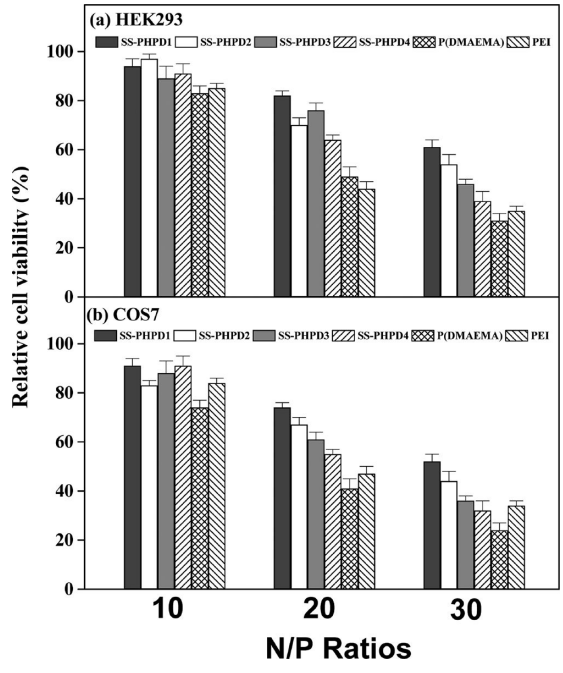

Figure 10. Cell viability of polymer/pDNA complexes at different N/P ratios in (a) HEK293 and (b) COS7 cell lines.

dx.doi.org/10.1021/am400022q | ACS Appl. Mater. Interfaces 2013, 5, 1840−1848

polymer, besides the compact and positively charged polymer/pDNA complexes. The increased free cationic polymers produced the increasing cytotoxicity. At the same N/P ratio, the cell viability seemed to be highly dependent on the P(DMAEMA) side chain length. SS-PHPD4 with the longest P(DMAEMA) side chains seems to be the most toxic. It was well-known that the cytotoxicity of polycations increases with the molecular weight.[29] Because of the increased length in the P(DMAEMA) side chains of SS-PHPD1 to SS-PHPD4, their cytotoxicity shows the general upward trend as expected. The cytotoxicity of SS-PHPDs could be controlled by adjusting the length of the P(DMEAMA) side chains.

In vitro Gene Transfection Assay. The in vitro gene transfection efficiency of the cationic polymer/pDNA complexes was first assessed using luciferase as a gene reporter in HEK293 and COS7 cell lines in the complete serum media. Figure 11 shows the gene transfection efficiencies mediated by

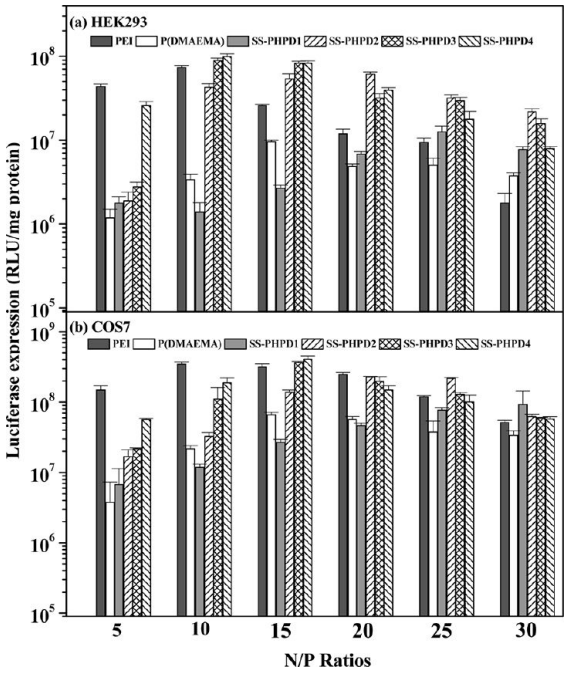

Figure 11. In vitro gene transfection efficiency of the cationic polymer (PEI (25 KDa), PHPD1, PHPD2, PHPD3, and PHPD4)/pDNA complexes at various N/P ratios in the presence of serum in (a) HEK293 and (b) COS7 cells.

SS-PHPDs at various N/P ratios in comparison with those of the control PEI (25 kDa) and P(DMAEMA) homopolymers. The transfection efficiency generally first increases at lower N/P ratios and then decreases slightly with the increase in N/P ratios. At lower N/P ratios, pDNA cannot be condensed efficiently by the cationic polymers, and the resultant loose polymer/pDNA complex cannot enter the cell easily. At higher N/P ratios, the transfection formulation contain also free polymer. Due to the presence of an increasing amount of free cationic polymers with the increase in N/P ratios, the increasing cytotoxicity may result in a reduction in the transfection efficiency. In particular, the transfection efficiencies mediated by P(DMAEMA) and PEI in HEK293 cell lines (Figure 11a) decreases dramatically with the increase in the N/P ratios, presumably due to the high cytotoxicity of the two polymers.

The transfection efficiencies mediated by SS-PHPD1 were significantly lower than those mediated by other SS-PHPDs at various N/P ratios, indicating that the transfection efficiency for SS-PHPDs was dependent on the side lengths of P(DMAEMA). With the increase in the side chain length of P(DMAEMA) of SS-PHPDs, their optimal transfection efficiency generally increases in the two cell lines. The long P(DMAEMA) side chains can increase the binding ability and complex stability, probably leading to a much higher transfection efficiency. The transfection efficiency mediated by SS-PHPD2 to SS-PHPD4 is much higher than that mediated by the control P(DMAEMA) homopolymer. The averaged number of DMAEMA repeat units per side chain of SS-PHPD2 to SS-PHPD4 (Table 1) is much lower than that (about 180) of the P(DMAEMA) homopolymer, indicating that the high-molecular-weight comb copolymers composed of degradable PHPA backbones and disulfide-linked low-molecular-weight P(DMAEMA) side chains can enhance gene transfection efficiency. As mentioned above, the disulfide bridge linkages were responsive to the reductive agent, making SS-PHPDs breakable. Under intracellular reducible conditions, such responsiveness could lead the unstable complexes, which were readily decondensed to greatly facilitate pDNA release from the complexes and benefit the resultant gene expression.

CONCLUSIONS

The bioreducible ATRP initiation sites have been successfully introduced onto PHPA backbones. A series of new well-defined comb-shaped vectors (SS-PHPDs) with different lengths of disulfide-linked cationic P(DMAEMA) side chains were subsequently prepared from the bromoisobutyryl-terminated PHPA biopolymers. The P(DMAEMA) side chains were readily cleavable from the backbones under reducible conditions. The degradability of PHPA backbones would benefit the final removal of the gene carriers from the body. More importantly, such comb-shaped SS-PHPD vectors could exhibit the good pDNA condensation ability, low cytotoxicity and enhanced gene transfection efficiencies in different cell lines. The bioreducible and biodegradable properties of the SS-PHPD vectors would make them have great potential as promising candidates for future in vivo gene therapy applications.

AUTHOR INFORMATION

Corresponding Author

*E-mail: xufj@mail.buct.edu.cn.

Notes

The authors declare no competing financial interest.

ACKNOWLEDGMENTS

This work was supported by National Natural Science Foundation of China (grant numbers 21074007, 51173014, and 51221002), Research Fund for the Doctoral Program of Higher Education of China (project no. 20120010110007), Program for New Century Excellent Talents in University (NCET-10-0203), SRF for ROCS, SEM and National High Technology Development Program of China (863 Program 2011AA030102).

REFERENCES

(1) Tian, H. Y.; Lin, L.; Chen, J.; Chen, X. S.; Park, T. G.; Maruyama, A. *J. Controlled Release* **2011**, *1*, 47−53.

(2) Lee, Y.; Lee, S. H.; Kim, J. S.; Maruyama, A.; Chen, X. S.; Park, T. G. *J. Controlled Release* **2011**, *155*, 3−10.
(3) Wang, H. Y.; Yi, W. J.; Qin, S. Y.; Li, C.; Zhuo, R. X.; Zhang, X. Z. *Biomaterials* **2012**, *33*, 8685−8694.
(4) Xu, F. J.; Yang, W. T. *Prog. Polym. Sci.* **2011**, *36*, 1099−1131.
(5) Lin, C.; Blaauboer, C. J.; Mateos Timoneda, M.; Lok, M. C.; van Steenbergen, M.; Hennink, W. E.; Zhong, Z. Y.; Feijen, J.; Engbersen, J. F. J. *J. Controlled Release* **2008**, *126*, 166−174.
(6) Luo, K.; Li, C. X.; Li, L.; She, W. C.; Wang, G.; Gu, Z. W. *Biomaterias* **2012**, *33*, 4917−4927.
(7) Mao, S.; Sun, W.; Kissel, T. *Adv. Drug Delivery Rev.* **2010**, *62*, 12−27.
(8) Ortiz Mellet, C.; García Fernández, J. M.; Benito, J. M. *Chem. Soc. Rev.* **2011**, *40*, 1586−1608.
(9) Ping, Y.; Liu, C. D.; Tang, G. P.; Li, J. S.; Li, J.; Yang, W. T.; Xu, F. J. *Adv. Funct. Mater.* **2010**, *20*, 3106−3116.
(10) Xu, F. J.; Ping, Y.; Ma, J.; Tang, G. P.; Yang, W. T.; Kang, E. T.; Neoh, K. G. *Bioconjug. Chem.* **2009**, *20*, 1449−1458.
(11) Wang, Z. H.; Li, W. B.; Ma, J.; Tang, G. P.; Yang, W. T.; Xu, F. J. *Macromolecules* **2011**, *44*, 230−239.
(12) Chen, D.; Ping, Y.; Tang, G. P.; Li, J. *Soft Matter* **2010**, *6*, 955−964.
(13) Siegwart, D. J.; Oh, J. K.; Matyjaszewski, K. *Prog. Polym. Sci.* **2011**, *37*, 18−37.
(14) Xu, F. J.; Zhu, Y.; Liu, F. S.; Nie, J.; Ma, J.; Yang, W. T. *Bioconjug. Chem.* **2010**, *21*, 456−464.
(15) Bontempo, D.; Leonardis, P. D.; Mannina, L.; Capitani, D.; Crescenzi, V. *Biomacromolecules* **2006**, *7*, 2154−2161.
(16) Dupayage, L.; Save, M.; Dellacherie, E.; Nouvel, C.; Six, J. L. *J. Polym. Sci., Part A: Polym. Chem.* **2008**, *46*, 7606−7620.
(17) Tsarevsky, N. V.; Matyjaszewski, K. *Macromolecules* **2005**, *38*, 3087−3092.
(18) Li, Y.; Armes, S. P. *Macromolecules* **2005**, *38*, 8155−8162.
(19) Dai, F.; Sun, P.; Liu, Y.; Liu, W. *Biomaterials* **2010**, *31*, 559−569.
(20) Zhang, G. Y.; Liu, J.; Yang, Q. Z.; Zhou, R. X.; Jiang, X. L. *Bioconjugate Chem.* **2012**, *23*, 1290−1299.
(21) Meng, F.; Hennink, W. E.; Zhong, Z. Y. *Biomaterials* **2009**, *30*, 2180−2198.
(22) Wang, Z. H.; Zhu, Y.; Chai, M. Y.; Yang, W. T.; Xu, F. J. *Biomaterials* **2012**, *33*, 1873−1883.
(23) Kang, H. C.; Kang, H. J.; Bae, Y. H. *Biomaterials* **2011**, *32*, 1193−1203.
(24) Licciardi, M.; Campisi, M.; Cavallaro, G.; Cervello, M.; Azzolina, A.; Giammona, G. *Biomaterials* **2006**, *27*, 2066−2075.
(25) Cavallaro, G.; Scire, S.; Licciardi, M.; Ogris, M.; Wagner, E.; Giammona, G. *J. Controlled Release* **2008**, *131*, 54−63.
(26) Xue, W.; Diao, H.; Chen, X.; Wang, C.; Chen, J.; Zhang. *J. Eur. J. Pharm. Biopharm.* **2008**, *66*, 327−333.
(27) Tang, G. P.; Zhu, K. J.; Chen, Q. Q. *J. Appl. Polym. Sci.* **2000**, *77*, 2411−2417.
(28) Tang, L. Y.; Wang, Y. C.; Li, Y.; Du, J. Z.; Wang, J. *Bioconjugate Chem.* **2009**, *20*, 1095−1099.
(29) Wetering, P. V. D.; Moret, E. E.; Nieuwenbroek, N. M. E.; Steenbergen, M. J. V.; Hennink, W. E. *Bioconjugate Chem.* **1999**, *10*, 589−597.